J. W. Baish
Department of Mechanical Engineering and Applied Mechanics.

K. R. Foster
Department of Bioengineering.

P. S. Ayyaswamy
Department of Mechanical Engineering and Applied Mechanics, Mem. ASME

University of Pennsylvania, Philadelphia, Pa. 19104

Perfused Phantom Models of Microwave Irradiated Tissue

The theoretical basis, practical design considerations, and prototype testing of a perfused model suitable for simulation studies of microwave heated tissue are presented. A parallel tube heat exchanger configuration is used to simulate the internal convection effects of blood flow. The global thermal response of the phantom, on a scale of several tube spacings, is shown theoretically to be nearly identical to that predicted by Pennes' bioheat equation, which is known to give a reasonable representation of tissue under many conditions. A parametric study is provided for the relationships between the tube size, spacing and material properties and the simulated perfusion rate. A prototype with a physiologically reasonable perfusion rate was tested using a typical hyperthermia applicator. The measured thermal response of the phantom compares favorably with the numerical solution of the bioheat equation under the same irradiation conditions. This similarity sheds light on the unexpected success of the bioheat equation for modeling the thermal response of real tissue.

Introduction

The use of electromagnetic tissue-equivalent physical materials, called phantoms, is well established in hyperthermia research for estimating the power deposition patterns in treated tissue. In this paper a "dynamic" phantom is described that has microwave absorption and thermal diffusion properties that are both similar to those of living tissue and convective heat clearance properties similar to that modeled in the bioheat transfer equation (BHTE) [1]

$$\nabla \cdot (k_t \nabla T_t) - W_b (T_t - T_a) + q_t = \rho_t c_t \frac{\partial T_t}{\partial t} \tag{1}$$

where T_t is the local average tissue temperature, k_t is the tissue thermal conductivity, W_b is a perfusion rate dependent parameter, T_a is the arterial supply temperature (generally assumed to be constant), q_t is the volumetric heat generation rate, ρ_t is the effective density of the tissue, c_t is the effective specific heat of the tissue and t is the time. We chose this formulation because it qualitatively describes tissue reasonably well and it provides an adjustable parameter W_b that has been identified with the blood perfusion rate in real tissues [2, 3].

Despite its apparent empirical success, the BHTE has been criticized on theoretical grounds. Originally the heat sink term in the BHTE was assumed to arise from the thermal equilibration of the blood in the capillary bed with the surrounding tissue. Recent studies, that rigorously relate the blood-tissue heat transfer to the vascular organization in tissues, have shown that blood thermally equilibrates in relatively large countercurrent vessels [4, 5]. They suggest that the BHTE seems to work only because it provides enough adjustable parameters to fit the available data.

The present phantom model has a flow geometry quite different from the microcirculatory geometry in tissue, yet is closely described in its thermal response by the BHTE. The model helps provide insight into the apparently surprising success of the BHTE.

Description of the Phantom

The phantom consists of a solid matrix of electromagnetic tissue-equivalent material in which a parallel array of tubes is embedded (Fig. 1). Water passed rapidly through these tubes can simulate the convective cooling effects of the blood perfusion in tissue. The matrix itself has bulk electrical and thermal properties that are similar to those of tissue. Since the fraction

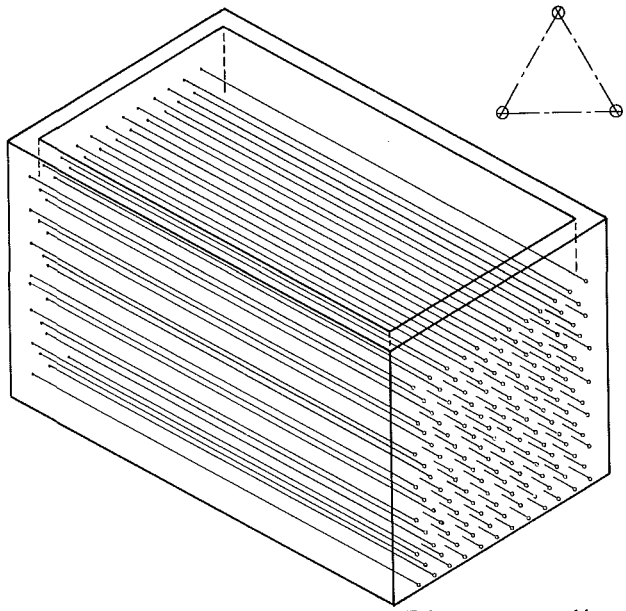

Fig. 1 Configuration of tubes in the phantom. Tubes are arranged in a parallel array on equilateral triangular centers.

Contributed by the Bioengineering Division for publication in the JOURNAL OF BIOMECHANICAL ENGINEERING. Manuscript received by the Bioengineering Division, July 26, 1985; revised manuscript received March 14, 1986.

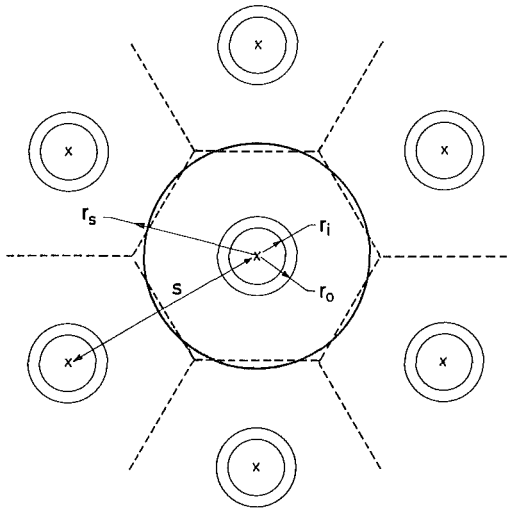

Fig. 2 Region adjacent to a typical tube. The local average temperature is the area average of the shaded region.

of the total volume occupied by the tubes is only a few percent, the bulk properties of the model are little affected by their presence.

We will demonstrate that heat clearance in the phantom is closely approximated by a relation analogous to the BHTE

$$\nabla \cdot (k_p \nabla T_p) - W_p (T_p - T_o) + q_p = \rho_p c_p \frac{\partial T_p}{\partial t} \tag{2}$$

where T_p is the local average phantom temperature, k_p is the matrix conductivity (matched to that of tissue), W_p is the strength of the heat sink per unit volume per unit temperature elevation (matched to W_b) and T_o is the cooling water temperature (matched to T_a). A high coolant flowrate can assure that the coolant will remain at an essentially constant temperature along the length of the tubes. (Subsequently, all temperatures will be referenced to T_o or T_a as appropriate.) The difference between the reference temperature and the local temperature in the solid matrix will simulate the difference between the tissue and arterial temperatures in the BHTE.

Two length scales exist in the phantom: the local scale, that applies to the region from a particular tube to the midpoint between tubes, and the global scale, pertaining to distances of several tube spacings. In use, the phantom will have temperature sensors located only between the tubes, so we consider the local average temperature in equation (2) to be defined as

$$T_p = \frac{1}{A} \int_A T dA \tag{3}$$

where A is the area of the hexagonal region around a tube less the area of the tube (Fig. 2). (The hexagonal boundary results from symmetry due to the equilateral triangular pattern of tubes.) The averaging in equation (3) takes place over only the region from the outside of the tube to the outer boundary of the local region; the region inside the circle of radius r_o has been excluded.

There are some important differences between the phantom and a system that exactly satisfies the BHTE. In the BHTE the rate at which heat is drawn into the arterial temperature heat sink is proportional to the blood perfusion rate and the temperature elevation. In contrast, in the phantom the rate of heat removal by the coolant tubes depends on the thermal resistance between the coolant in the tubes and the solid matrix. As long as the flowrate is high enough to avoid temperature increases in the direction of flow the simulated perfusion rate is independent of the flowrate and depends only on the dimensions and material properties of the tubes and matrix.

Design Analysis

To demonstrate similitude between the phantom and the BHTE we must show that the heat sink is isotropic and that W_p can be determined from the tube spacing, tube diameter, tube wall thickness and thermal properties. The isotropic nature of the heat sink might seem surprising in view of the directional flow of coolant in the tubes, but will be shown to

Nomenclature

A = area of hexagonal region around tube
a_n, a_n' = constant coefficients of separation of variables solution
b_n, b_n' = constant coefficients of separation of variables solution
c_b = specific heat of blood
c_p = specific heat of phantom material
c_t = specific heat of tissue being simulated
c_w = specific heat of water
$G(t)$ = function of t alone from separation of variables
g = acceleration of gravity
H = equivalent heat transfer coefficient based on outer radius of tube
h = heat transfer coefficient inside tube
$J_n(r)$ = Bessel function of first kind order n argument r
k_p = thermal conductivity of phantom material
k_t = thermal conductivity of tissue being simulated
k_{tube} = thermal conductivity of tube
k_w = thermal conductivity of water
L = length of tube
m = mass flowrate per tube
Nu = Nusselt number
Q = volume flowrate of water per tube
q_p = volumetric heat generation rate in phantom
q_t = volumetric heat generation rate in tissue
$R(r)$ = function of r alone from separation of variables
r = radial coordinate measured from center of tube
r_i = inner radius of tube
r_o = outer radius of tube
r_s = radius of symmetry between tubes
T_a = arterial supply temperature in tissue
T_o = temperature of heat sink in phantom
T_p = local average temperature in phantom
T_t = tissue temperature
t = time
W_b = perfusion rate-dependent heat sink strength in tissue
w_b = perfusion rate in tissue
W_p = heat sink strength in phantom
x = coordinate normal to tubes and to y-axis
$Y_n(r)$ = Bessel function of second kind order n argument r
y = coordinate normal to tubes and to x-axis
$Z(z)$ = function of z alone from separation of variables
z = coordinate parallel to tubes
α = thermal diffusivity
β = eigenvalue
θ = azimuthal position with respect to tube
ν = kinematic viscosity of water
ρ = density of water

be a close approximation when the flowrate is high in the tubes.

To simplify the analysis, the BHTE and the phantom equation will be considered term by term in the following four parts: 1) the steady-state balance of the heat generation term with the heat sink in the absence of diffusion; 2) the steady-state balance of conduction in the direction transverse to the tubes with the heat sink; 3) the steady-state balance of conduction in the direction parallel to the tubes with the heat sink; 4) and the transient balance of the sensible energy storage term and the heat sink. Complications arising from boundary and initial conditions are avoided by assuming that the heated region is small compared to the total volume of the model and that the initial temperature is uniform throughout the phantom. Each part of the equation will yield an estimate of W_p that will later be shown to be nearly identical despite their different mathematical forms and physical origins.

1 Heat Generation. The first consideration is the balance of the heat generation and blood heat sink terms. Physically, this corresponds to a situation in which heat is generated uniformly throughout the medium and is removed by the nearest tube. If the heat generation rate is a constant (q_o) throughout a tissue and no large-scale conduction takes place, the BHTE predicts a steady-state temperature elevation of q_o/W_b.

We now consider how the local average temperature in the phantom can be made equal to this temperature. Symmetry requires that the hexagonal boundary around a typical tube as shown in Fig. 2 be adiabatic. Approximate analysis of this geometry can be carried out by replacing the hexagon by a circle of equal area (r_s = 1.907/s) so that the total heat generated in the phantom is accounted for.

The simulated perfusion rate for this case (W_{p1}) is found by solving the heat conduction equation in cylindrical coordinates

$$\frac{d^2T}{dr^2}+\frac{1}{r}\frac{dT}{dr}+\frac{q_o}{k_p}=0 \tag{4}$$

subject to the boundary conditions

$$\left.\frac{dT}{dr}\right|_{r=r_s}=0 \tag{5a}$$

$$HT(r_o)=k_p\left.\frac{dT}{dr}\right|_{r=r_o} \tag{5b}$$

The convection condition at the tube wall (equation (5b)) is based on an effective convection coefficient that includes effects from the thermal resistance of the tube wall and that between the tube wall and the mixed mean temperature of the coolant. The condition at the inside wall of the tube is

$$\frac{\mathrm{Nu}k_w}{2r_i}T(r_i)=k_{\text{tube}}\left.\frac{dT}{dr}\right|_{r=r_i} \tag{6}$$

where the Nusselt number Nu is $2r_ih/k_w$ and assumed equal to 48/11 for the design analysis. This corresponds to the case when the heat flux is uniform along the length of the tube [6]. The thermal resistance of the tube wall can be added in series to that of the coolant to give the effective convection coefficient

$$H=\left[\frac{2r_o}{\mathrm{Nu}k_w}+\frac{r_o}{k_{\text{tube}}}\ln\left(\frac{r_o}{r_i}\right)\right]^{-1} \tag{7}$$

The solution of the foregoing boundary value problem is

$$T(r)=\frac{q_o}{2k_p}\left\{\frac{r_o^2-r^2}{2}+\frac{r_ok_p}{H}\left[\left(\frac{r_s}{r_o}\right)^2-1\right]+r_s^2\ln\left(\frac{r}{r_o}\right)\right\} \tag{8}$$

The local phantom temperature T_p is found from the integral

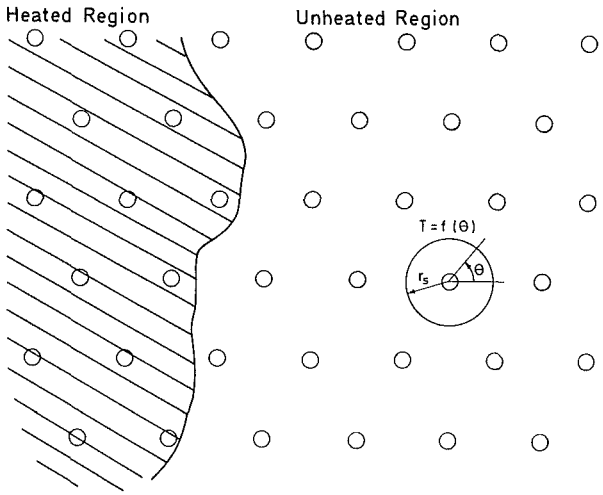

Fig. 3 Conditions for transverse conduction

$$T_p=\frac{2}{r_s^2-r_o^2}\int_{r'=r_o}^{r_s}T(r')r'dr' \tag{9}$$

which yields

$$T_p=\frac{q_o}{k_r(r_s^2-r_o^2)}\left\{\left(\frac{r_o^2-r_s^2}{4}+\frac{r_ok_p}{2H}\left[\left(\frac{r_s}{r_o}\right)^2-1\right]-\frac{r_s^2}{2}\ln r_o\right)(r_s^2-r_o^2)+\frac{r_s^2}{2}(r_s^2\ln r_s-r_o^2\ln r_o)+\frac{r_o^4-r_s^4}{8}\right\} \tag{10}$$

This provides a local temperature increase from which, by comparison with that obtained from the BHTE, the simulated perfusion rate can be obtained.

2 Transverse Conduction. When there is a global temperature gradient normal to the tubes, the phantom must remove heat at a rate $W_bT_t = W_{p2}T_p$ if it is to match the BHTE. We analyze this condition by considering the heat removed by a tube outside of the region of heat generation (Fig. 3). In general, the temperature at r_s is a function of the aximuthal position.

To evaluate W_{p2} we solve Laplace's equation in cylindrical coordinates with both angular and radial dependence

$$\frac{\partial^2T(r,\theta)}{\partial r^2}+\frac{1}{r}\frac{\partial T(r,\theta)}{\partial r}+\frac{1}{r^2}\frac{\partial^2T(r,\theta)}{\partial\theta^2}=0 \tag{11}$$

subject to

$$T(r_s,\theta)=f(\theta) \tag{12a}$$

$$HT(r_o,\theta)=k_p\left.\frac{\partial T}{\partial r}\right|_{r=r_o,\theta} \tag{12b}$$

with $T(r, \theta)$ periodic with period 2π. If we assume that $T(r, \theta) = \Theta_n(\theta)R_n(r)$, equation (11) separates into two ordinary differential equations

$$\frac{d^2}{dr^2}R(r)+\frac{1}{r}\frac{d}{dr}R(r)+\frac{\nu^2}{r^2}R(r)=0 \tag{13a}$$

and

$$\frac{d^2\Theta(\theta)}{d\theta^2}+\nu^2\Theta(\theta)=0 \tag{13b}$$

The general solution will have the form

$$T(r,\theta)=a_o+a_o'\ln r+\sum_{n=1}^{\infty}(a_nr^{2\pi n}+a_n'r^{-2\pi n})(b_n\cos(2\pi n\theta)+b_n'\sin(2\pi n\theta)) \tag{14}$$

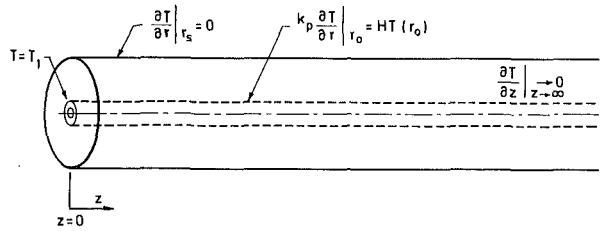

Fig. 4 Conditions for axial conduction

where the a_n, a_n', b_n, and b_n' are constants determined by the boundary conditions. The local average temperature in the solid matrix is

$$T_p=\frac{1}{\pi(r_s^2-r_o^2)}\int_{r=r_o}^{r_s}\int_{\theta=0}^{2\pi}T(r,\theta)rdrd\theta \tag{15}$$

Substituting equation (14) and integrating gives

$$T_p=a_o-\frac{a_o'}{2}+a_o\left[\frac{r_s^2\ln r_s-r_o^2\ln r_o}{r_s^2-r_o^2}\right] \tag{16}$$

where integrals over $\sin(2\pi n\theta)$ and $\cos(2\pi n\theta)$ vanish.

The heat removed by the tube per unit length can be written as

$$r_o k_p\int_{\theta=0}^{2\pi}\frac{\partial T}{\partial r}\Big|_{r_o,\theta}d\theta=2\pi k_p a_o' \tag{17}$$

or

$$r_o H\int_{\theta=0}^{2\pi}T(r_o,\theta)d\theta=2\pi r_o H(a_o+a_o'\ln r_o) \tag{18}$$

where in both cases the angular terms again make no contribution. Thus the heat removed and T_p do not depend on the angular dependence of the outer boundary condition.

To find the full set of coefficients $f(\theta)$ must be represented as a Fourier series. Here we require only the zeroth-order terms, which must satisfy

$$a_o+a_o'\ln r_s=\frac{1}{2\pi}\int_{\theta=0}^{2\pi}f(\theta)d\theta \tag{19}$$

where the integral is just the angular average of the outer boundary temperature which we define as T_s. By applying equations (17), (18) and (19), we find the necessary coefficients are

$$a_o=T_s-a_o'\ln r_s \tag{20a}$$

$$a_o'=\frac{HT_s}{\frac{k_p}{r_o}+H\ln\left(\frac{r_s}{r_o}\right)} \tag{20b}$$

In comparison with the BHTE, the heat removed per unit volume is $W_{p2}T_p$, so the second expression for the phantom perfusion rate can be found from

$$W_{p2}=\frac{2k_p a_o'}{(r_s^2-r_o^2)T_p} \tag{21}$$

from which T_s can be eliminated.

3 Axial Conduction. Next we consider the case where heat is globally conducted parallel to the tubes. Before analyzing the phantom we look first at how the BHTE would respond under similar circumstances. We consider a region of tissue in which no heat generation takes place but that has a temperature elevation due to a heat source elsewhere. If the temperature varies only in one direction and if the temperature is T_1 at a plane $z = 0$, then the BHTE will predict a temperature decay according to

$$T_t(z)=T_1\exp(-z\sqrt{W_b/k}) \tag{22}$$

The phantom must simulate this exponential behavior and its simulated perfusion rate is based on the decay constant of the exponential.

Figure 4 shows the vicinity of a typical tube in this situation. Heat conducting from the end at T_1 can either be conducted immediately into the tube or be conducted down the length of the tube to be absorbed by the tube at some later point. In order to determine the length scale over which heat is conducted into the tube we consider the heat conduction equation

$$\frac{\partial^2 T(r,z)}{\partial r^2}+\frac{1}{r}\frac{\partial T(r,z)}{\partial r}+\frac{\partial^2 T(r,z)}{\partial z^2}=0 \tag{23}$$

subject to

$$T(r,o)=T_1 \tag{24a}$$

$$T(r,\infty)\text{ bounded} \tag{24b}$$

$$\frac{\partial T}{\partial r}\Big|_{r_s,z}=0 \tag{24c}$$

$$HT(r_o,z)=k_p\frac{\partial T}{\partial r}\Big|_{r_o,z} \tag{24d}$$

The radial boundary conditions are the same as in the first case.

Proceeding with a separation of variables solution, we assume that the solution can be written as the product, $T(r,z) = R_n(r)Z_n(z)$. This allows the separation into two ordinary differential equations

$$\frac{d^2R_n(r)}{dr^2}+\frac{1}{r}\frac{dR_n(r)}{dr}+\beta_n^2R_n(r)=0 \tag{25a}$$

and

$$\frac{d^2Z_n(z)}{dz^2}-\beta_n^2Z_n(z)=0 \tag{25b}$$

Equations (25*a*) and (25*b*) admit solutions $J_o(\beta_n r)$ and $Y_o(\beta_n r)$, and $\exp(+z\beta_n)$ and $\exp(-z\beta_n)$, respectively. The positive exponent must be rejected because it diverges at infinity. The radial boundary conditions indicate which eigenvalues are appropriate. These are the real roots of

$$k_p\beta_n\left[J_1(\beta_n r_o)-\frac{J_1(\beta_n r_s)}{Y_1(\beta_n r_s)}Y_1(\beta_n r_o)\right]$$
$$+H\left[J_o(\beta_n r_o)+\frac{J_1(\beta_n r_s)}{Y_1(\beta_n r_s)}Y_o(\beta_n r_o)\right]=0 \tag{26}$$

The general temperature solution is the summation over all simple solutions, given by

$$T(r,z)=\sum_{n=1}^{\infty}(A_nJ_o(\beta_n r)+B_nY_o(\beta_n r))\exp(-\beta_n z) \tag{27}$$

The constants A_n and B_n can be determined by the boundary conditions but are not needed here, since we need only show that the leading behavior of the solution is exponential. The local average phantom temperature can be expressed as

$$T_p=\sum_{n=1}^{\infty}\left[\frac{2}{(r_s^2-r_o^2)}\int_{r=r_o}^{r_s}[A_nJ_o(\beta_n r)+B_nY_o(\beta_n r)]rdr\exp(-\beta_n z)\right] \tag{28}$$

Note that since we are averaging only in the r direction, the z and r dependence is still separable. If the second and higher order eigenfunctions decay sufficiently faster than the first then the response to a plane source is proportional to $\exp(-\beta_1 z)$ to a high degree of accuracy. When typical design values for the parameters are introduced, the first 8 eigenvalues may be found and are presented in Table 1. The first eigenvalue gives a good indication of the behavior of the phantom, since the second eigenvalue is more than five times the

Table 1 Eigenvalues for equation (26) assuming baseline design parameters

n	Eigenvalue (m^{-1})
1	117
2	649
3	1157
4	1674
5	2198
6	2725
7	3255
8	3787

Table 2 Baseline design parameters

Parameter	Symbol	Value
Phantom conductivity	k_p	0.60 W/m-C
Water conductivity	k_w	0.60 W/m-C
Tube conductivity	k_{tube}	0.25 W/m-C
Phantom specific heat	c_p	4184 J/Kg-C
Blood specific heat	c_b	4184 J/Kg-C
Tube inner radius	r_i	0.635 mm
Tube outer radius	r_o	1.143 mm
Radius of symmetry	r_s	7.000 mm

value with the decay constant found from the BHTE. Thus we find W_{p3} is $k\,\beta_1^2$.

4 Transient Response. The simplest balance of terms in the BHTE that will demonstrate the transient response is the case where the phantom is initially at a uniform temperature elevation T_1 and is allowed to decay to the reference temperature. The solution of the BHTE under these conditions is

$$T_t = T_1 \exp\left(\frac{-W_B}{\rho_t c_t}\, t\right) \tag{29}$$

where we see that the time constant is perfusion dependent.

Since the initial temperature is uniform throughout, the same symmetry that was used for the first criterion can be used in this analysis also. The boundary/initial value problem to be solved on the local scale in the phantom is

$$\frac{\partial^2 T(r,t)}{\partial r^2} + \frac{1}{r}\frac{\partial T(r,t)}{\partial r} = \frac{1}{\alpha}\frac{\partial T(r,t)}{\partial t} \tag{30}$$

subject to

$$\left.\frac{\partial T}{\partial r}\right|_{r_s,t} = 0 \tag{31a}$$

$$HT(r_o,t) = k_p \left.\frac{\partial T}{\partial r}\right|_{r_o,t} \tag{31b}$$

and initial condition

$$T(r,\theta) = T_1 \tag{31c}$$

Separating variables such that $T(r, t) = R_n(r)G_n(t)$, we find the two ordinary differential equations that apply

$$\frac{d^2 R_n(r)}{dr^2} + \frac{1}{r}\frac{dR_n(r)}{dr} + \beta_n^2 R_n(r) = 0 \tag{32a}$$

and

$$\frac{dG_n(t)}{dt} = -\alpha\beta_n^2 G_n(t) \tag{32b}$$

The time-dependent variable admits solutions of the form $\exp(-\,t\alpha\beta_n^2)$ where the positive exponent has been ignored because it diverges for long times. The radial solutions are of the form $J_o(\beta_n r)$ and $Y_o(\beta_n r)$ and must satisfy the same boundary conditions as the radial solution for axial conduction. Therefore, the eigenvalues are the same as those found from the solutions of equation (29). If we equate the time constants from the BHTE and the phantom we find that W_{p4} is $k\,\beta_1^2$, the same as the axial flow criterion with the same limitations. All higher order eigenvalues have been suppressed. In the transient case these correspond to time constants that are

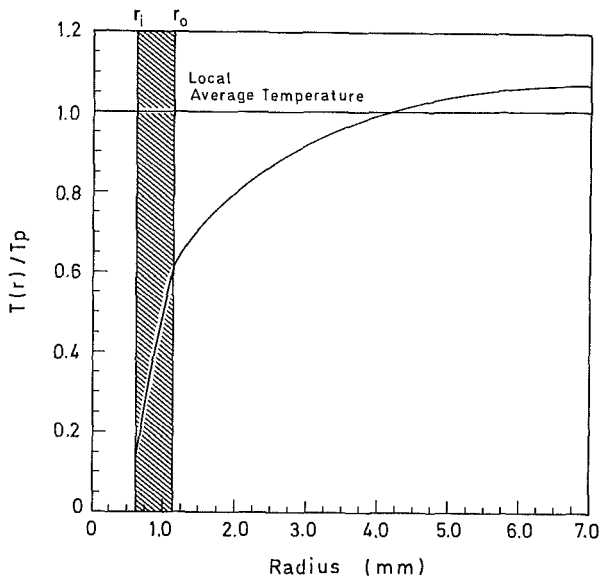

Fig. 5 Local temperature gradients in the vicinity of a typical tube

at least 25 times greater than the slowest time constant. Physically, this means that the phantom very quickly reaches a quasi-steady condition where the temperature profile between the tubes is of constant shape but continually decreases in magnitude.

Local Temperature Gradients

The analysis so far has been oriented toward demonstrating that the local average temperature approximates solutions to the BHTE. An important consideration is the difference between the maximum temperature at the hot spot between the tubes and the temperature at the outer tube wall or the local average temperature (Fig. 5). Most applications of the phantom will use sensors such as thermistors or thermocouples that sample a much smaller volume than would be necessary to give a good indication of the local average temperature. The temperature drop between the phantom hot spot (located at $r = r_s$) and the coolant can take place in three regions: the solid matrix, the tube wall or the fluid itself. If the major temperature drop occurs in the solid matrix large errors are possible if the sensor is randomly placed in the matrix at an unknown distance from the tubes. The error can be corrected by knowing the exact location of each sensor with respect to the tubes (for example, the midpoint between neighboring tubes). Alternatively, the phantom can be designed so that the exact location of a sensor is not critical. This is done by placing the largest thermal resistance either in the tube wall or in the fluid. Since the convection coefficient is not well known or controllable, it is preferable to design the phantom so that the major temperature drop is across the tube wall. The ratio of the local maximum temperature to the local minimum temperature (located at $r = r_o$) will be calculated in the following parametric study as a measure of the local temperature gradients. We also calculated the ratio of the maximum local temperature to the local average temperature for use as a correction factor for small sensors located at the midpoint between tubes.

Design Parameter Study

Now that three different criteria for the design of the phantom have been defined we consider what numerical values these take on for a range of realistic tube sizes and spacings. A set of baseline design parameters found in Table 2 are proposed for the design study. The effects of variation of individual parameters away from the design values will be investigated.

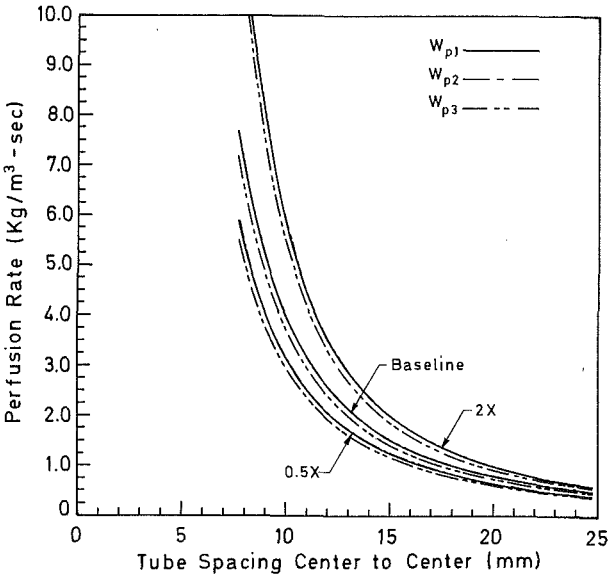

Fig. 6 Parametric dependence of the simulated perfusion rate on the tube spacing and tube size. The small difference between the various estimates of the simulated perfusion rate demonstrates that the phantom has a highly isotropic response. A constant ratio $r_o/r_i = 1.8$ is used.

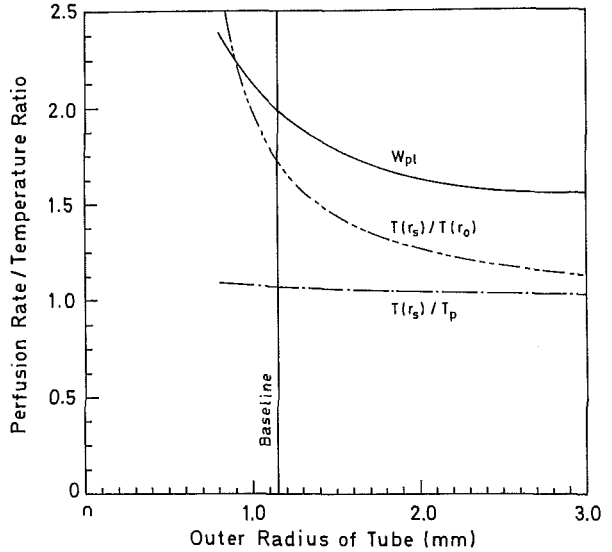

Fig. 7 Parametric dependence of the simulated perfusion rate on the tube wall thickness. The magnitude of the local gradients is also plotted. The advantage of a thick-walled tube for reducing the local gradients is demonstrated.

The property values given in Table 2 pertain to pure water and are not exact values for any particular tissue or blood. The values given however are sufficiently accurate for a design study.

We must first establish that the three design criteria give similar results, given the same input parameters. All three of the design criteria (W_{p1}, W_{p2}, and W_{p3}) are plotted in Fig. 6 and it can be seen that the differences in the three are minimal over a wide range of spacings and tube sizes. The difference between the design perfusion rates was never greater than a few percent. The similarity of W_{p2} and W_{p3} indicates that the phantom will have a highly isotropic response. The choice of which design criterion to employ is thus a matter of convenience since all three give essentially the same results.

The simulated perfusion rate was found to be most sensitive to the tube spacing, with a lesser dependence on the tube radius, for a constant ratio of outer to inner tube radius (Fig. 6). Variation of the tube wall thickness for a given outer radius is considered in Fig. 7. The impact of wall thickness is generally small on the simulated perfusion rate but the local

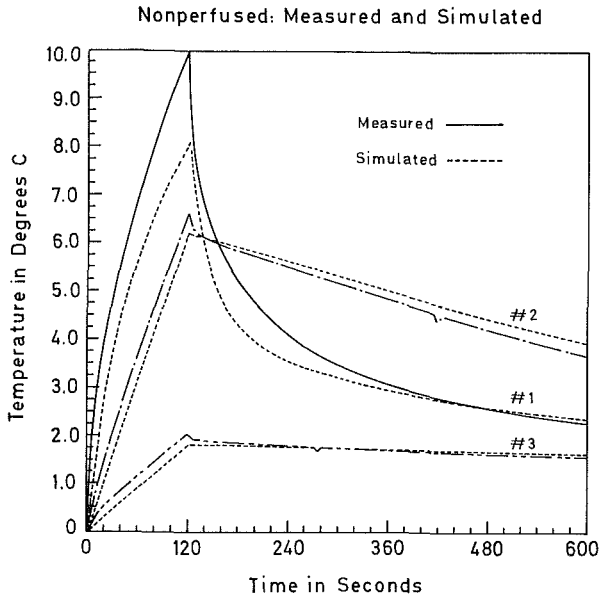

Fig. 8 Measured and predicted nonperfused response of three thermistors at depths of 0.1 cm (No. 1), 2.3 cm (No. 2), and 4.5 cm (No. 3) in the phantom filled with common gelatine (6 percent by weight). Heating with a 915-MHz 2.5 by 5 cm waveguide applicator for 120 s at about 20 W total absorbed power.

temperature gradients are undesirably large for very thin-walled tubes.

Design Realization

Several practical aspects of the design must also be considered. The pumping system and fixtures upstream from the tubes must be able to handle the flow resistance of the cooling water. Pressure head loss through tubes of length L can be estimated from [6]

$$h_L = \frac{8\nu LQ}{\pi g r_i^4} \tag{33}$$

where Q is the volume flowrate per tube. The flowrate in the phantom must be high enough to prevent a significant temperature rise along the length of the tube. This temperature rise under steady conditions for a given flowrate, heated region of width b, and heat generation rate q_o is given by

$$\Delta T = \frac{\pi b r_s^2 q_o}{\rho_w c_w Q} \tag{34}$$

For instance, if a region 5 cm wide lying normal to the tubes on the baseline spacing is heated at a uniform 100,000 W/m^3, then the flowrate must be 0.37 mL/s in each tube to limit the temperature rise in any tube from exceeding 0.5°C. The pressure drop through tubes of baseline size at this flowrate would be about 0.6 m of water per m of tube.

The total number of tubes must be also limited, if only by the perserverence of the person constructing the phantom. The prototype used 144 tubes which gave a perfused region measuring about 15 cm on a side.

Experimental Validation of the Prototype Dynamic Phantom

A prototype phantom built with the baseline design parameters (Table 2) was experimentally tested. The validation of this phantom consists of showing that the global thermal behavior is the same as predicted by the BHTE both with the simulated perfusion rate (2.0 kg/m^3-s) and with no perfusion. This procedure assures that the predictions of the phantom have an accurate quantitative interpretation in terms of the BHTE.

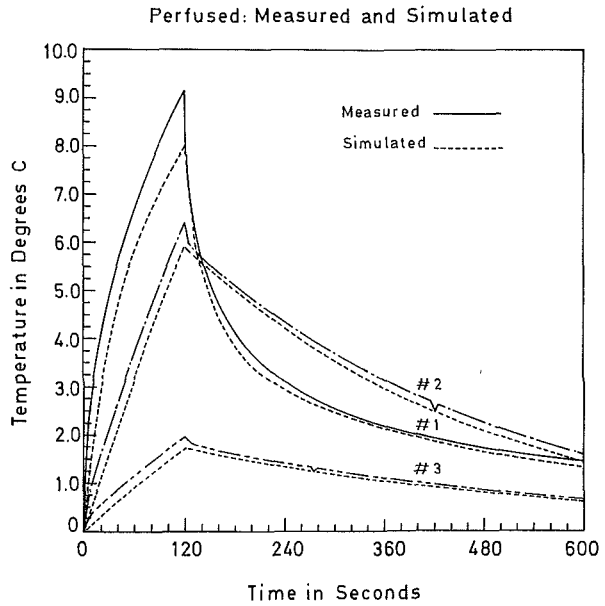

Fig. 9 Measured and predicted perfused response of three thermistors. Perfusion rate set at 2.0 kg/m^3·s in numerical simulation; equal to the design value for the phantom.

Validation of this design was accomplished by measuring the transient response of three-high resistance thermistors placed at depths of 0.1, 2.3 and 4.5 cm under the center axis of a typical hyperthermia applicator consisting of a section of a 2.5 by 5.0-cm ridged waveguide operating at 915 MHz. The heat generation pattern (i.e., specific absorption rate) was measured by the well-known split phantom thermographic technique [7].

A full three-dimensional and transient numerical simulation of the response of these thermistors was done by a finite difference solution to the BHTE assuming a heat input equal to the measured specific absorption rate. The predicted and measured response of the thermistors is shown in Fig. 8 for the nonperfused case. Figure 9 shows corresponding responses for the numerical model with a perfusion rate of 2.0 Kg/m^3-s and for the phantom with coolant flow. The favorable comparison indicates that the phantom behaves as planned.

Conclusions

The foregoing results show that a simple model can provide a useful thermal analog to the BHTE, and thus to a living tissue. Such a dynamic phantom can be useful for studying practical aspects of hyperthermia equipment performance that would not be anticipated with a purely numerical model.

The phantom design also sheds light on the apparent success of the BHTE itself. Its flow geometry bears little resemblence to the vascular geometry of tissue, yet its behavior is closely approximated by the BHTE. The highly directional flow in the poorly equilibrated tubes in the phantom produces an isotropic heat sink similar to that of the BHTE. The possibility arises that large, unequilibrated vessels in a real tissue might also act as line sinks, producing a thermal response that accidentally resembles that predicted by the BHTE. Since vessels with large flowrates should behave as a heat sink, regardless of their orientation, large countercurrent blood vessels would be expected to produce a heat sink as well. Smaller countercurrent vessels, that are nearly in thermal equilibrium with the surrounding tissue, have recently been shown to have an entirely different heat transfer mechanism (incomplete countercurrent exchange) and governing equation [5]. These vessels produce an apparent increase of the thermal conductivity of the tissue, instead of a heat sink. In a real tissue both heat transfer mechanisms are likely to be operating simultaneously. This situation might help to explain why it has been so difficult to agree on a suitable model for perfused tissue.

Simple physical models such as this phantom provide a well-controlled system in which to examine some of these fundamental issues of bioheat transfer. Their further study promises to contribute to a better understanding of real tissue.

Acknowledgments

This research was supported by NCI Grant CA-36624. The authors wish to thank Kenneth L. Carr of M/A-COM, Inc. for the use of the hyperthermia applicator and Dr. Gideon Kantor of the Bureau of Radiological Health for use of thermographic equipment used to determine the SAR for the hyperthermia applicator.

References

1 Pennes, H. H., "Analysis of Tissue and Arterial Blood Temperatures in the Resting Human Forearm," *Journal of Applied Physiology*, Vol. 1, 1948, pp. 93–122.

2 Perl, W., "An Extension of the Diffusion Equation to Include Clearance by Capillary Blood Flow," *Annals of New York Academy of Science*, Vol. 108, 1963, pp. 92–105.

3 Valvano, J. W., Allen, J. T., and Bowman, H. F., "The Simultaneous Measurement of Thermal Conductivity, Thermal Diffusivity, and Perfusion in Small Volumes of Tissue," ASME JOURNAL OF BIOMECHANICAL ENGINEERING, Vol. 106, 1984, pp. 192–196.

4 Weinbaum, S., Jiji, L. M., and Lemons, D. E., "Theory and Experiment for the Effect of Vascular Microstructure on Surface Tissue Heat Transfer—Part I: Anatomical Foundation and Model Conceptualization," ASME JOURNAL OF BIOMECHANICAL ENGINEERING, Vol. 106, 1984, pp. 321–330.

5 Weinbaum, S., and Jiji, L. M., "A New Simplified Bioheat Equation for the Effect of Blood Flow on Local Average Tissue Temperature," ASME JOURNAL OF BIOMECHANICAL ENGINEERING, Vol. 107, 1985, pp. 131–139.

6 Kays, W. M., and Crawford, M. E., *Convective Heat and Mass Transfer*, McGraw-Hill Book Co., New York, 1980.

7 Guy, A. W., "Analyses of Electromagnetic Fields Induced in Biological Tissues by Thermographic Studies on Equivalent Phantom Models," *IEEE Trans.*, Vol. MTT-19, 1971, pp. 205–215.